Cell Host & Microbe
Article

Super-Resolution Dissection of Coordinated Events during Malaria Parasite Invasion of the Human Erythrocyte

David T. Riglar,[1,2,5] Dave Richard,[1,5] Danny W. Wilson,[1,6] Michelle J. Boyle,[1,2,6] Chaitali Dekiwadia,[3] Lynne Turnbull,[4] Fiona Angrisano,[1] Danushka S. Marapana,[1] Kelly L. Rogers,[1] Cynthia B. Whitchurch,[4] James G. Beeson,[1,2] Alan F. Cowman,[1,2] Stuart A. Ralph,[3] and Jake Baum[1,2,*]
[1]The Walter and Eliza Hall Institute of Medical Research, Melbourne, Victoria 3052, Australia
[2]Department of Medical Biology
[3]Department of Biochemistry and Molecular Biology, Bio21 Molecular Science and Biotechnology Institute University of Melbourne, Melbourne, Victoria 3052, Australia
[4]The ithree Institute, University of Technology Sydney, Sydney, New South Wales 2007, Australia
[5]These authors contributed equally to this work
[6]These authors contributed equally to this work
*Correspondence: jake@wehi.edu.au
DOI 10.1016/j.chom.2010.12.003

SUMMARY

Erythrocyte invasion by the merozoite is an obligatory stage in *Plasmodium* parasite infection and essential to malaria disease progression. Attempts to study this process have been hindered by the poor invasion synchrony of merozoites from the only in vitro culture-adapted human malaria parasite, *Plasmodium falciparum*. Using fluorescence, three-dimensional structured illumination, and immunoelectron microscopy of filtered merozoites, we analyze cellular and molecular events underlying each discrete step of invasion. Monitoring the dynamics of these events revealed that commitment to the process is mediated through merozoite attachment to the erythrocyte, triggering all subsequent invasion events, which then proceed without obvious checkpoints. Instead, coordination of the invasion process involves formation of the merozoite-erythrocyte tight junction, which acts as a nexus for rhoptry secretion, surface-protein shedding, and actomyosin motor activation. The ability to break down each molecular step allows us to propose a comprehensive model for the molecular basis of parasite invasion.

INTRODUCTION

Few diseases have the global health and economic impact of malaria (Snow et al., 2005). The disease is caused by apicomplexan parasites from the genus *Plasmodium*, of which *P. falciparum* is associated with the majority of morbidity and mortality. In the human host, the asexual blood stage of the life cycle is responsible for all clinical symptoms. Over the ~48 hr cycle a single parasite grows and divides within an infected erythrocyte, giving rise to 16 or more merozoites, the smallest extracellular parasite form (~1–2 μm in length). These egress from the erythrocyte (Gilson and Crabb, 2009; Glushakova et al., 2005), dispersing to reinfect other erythrocytes. While the process of invasion is completed within seconds to minutes of egress (Dvorak et al., 1975; Gilson and Crabb, 2009), responses to merozoite antigens are an important component of human malarial immunity (Doolan et al., 2009). Consequently, the molecular events underlying erythrocyte invasion are key targets for both therapeutic and vaccine-based strategies to block parasite development (O'Donnell and Blackman, 2005; Richards and Beeson, 2009).

While the morphological stages of merozoite invasion were established 40 years ago by electron microscopy studies of simian and avian parasite species (Aikawa et al., 1978; Aikawa et al., 1981; Bannister et al., 1975; Ladda et al., 1969; Miller et al., 1979), to date no study has characterized these steps in human malaria parasites. Merozoite priming for invasion is likely set in motion after erythrocyte egress, with activation triggered by exposure to the ionic composition of blood plasma (Singh et al., 2010). Invasion then begins with a low-affinity attachment to the erythrocyte. This interaction is thought to be mediated by *m*erozoite surface *p*roteins (MSPs) (Cowman and Crabb, 2006), the most well characterized of which is the glycosylphosphatidyl inositol (GPI)-anchored MSP-1. The merozoite then reorientates so that its apical pole (site of the secretory organelles: the micronemes and rhoptries) contacts the erythrocyte surface (Aikawa et al., 1978; Dvorak et al., 1975; Gilson and Crabb, 2009). At this point, the merozoite appears irreversibly attached to the erythrocyte and committed to invasion. Active invasion proceeds through a depression in the erythrocyte surface, the invasion pit, followed by formation of a tight junction—a close apposition of parasite and erythrocyte plasma membranes (Aikawa et al., 1978; Bannister et al., 1975). The parasite's actomyosin motor (Baum et al., 2006b; Miller et al., 1979) then drives the merozoite inside. As the tight junction concurrently progresses rearwards, an electron dense fibrillar coat surrounding the merozoite is shed, suggesting proteolytic processing of the parasite surface (Aikawa et al., 1978; Ladda et al., 1969). Secretion of the lipid-rich rhoptry contents also occurs at this time (Bannister et al., 1986) and probably plays a key

role in establishing the parasitophorous vacuole membrane (PVM), which fuses to surround the invaded parasite (Lingelbach and Joiner, 1998).

Despite progress in dissecting the stages of invasion and identification of key proteins involved (reviewed in Cowman and Crabb, 2006) the molecular and cellular coordination of the process remains unknown. A protein that likely plays a central role is *a*pical *m*embrane *a*ntigen 1 (AMA1). This micronemal protein is well conserved across apicomplexans and is essential for parasite viability (Mital et al., 2005; Triglia et al., 2000). AMA1 may mediate apical reorientation (Mitchell et al., 2004), rhoptry secretion (Mital et al., 2005), and signaling events upstream of invasion (Leykauf et al., 2010; Treeck et al., 2009). Most recently, a role in tight-junction formation has also been suggested (Collins et al., 2009; Richard et al., 2010). This proposal follows studies with a related apicomplexan parasite *Toxoplasma gondii*, in which AMA1 was identified as partner to a complex containing *rh*optry *n*eck proteins (RONs) that localize to the tight junction during invasion (Alexander et al., 2005; Besteiro et al., 2009; Straub et al., 2009). At least two members of the RON complex, RON4 and RON5, have since been shown to translocate to the cytosolic side of the host cell plasma membrane during *T. gondii* invasion, where they may anchor the rest of the complex (Besteiro et al., 2009; Straub et al., 2009). Orthologs of these proteins have been identified in the malaria parasite and found to associate together in asexual stage protein extracts (Alexander et al., 2006; Cao et al., 2009; Collins et al., 2009; Richard et al., 2010). Furthermore, inhibition of the PfAMA1-RON interaction prevents merozoite invasion, demonstrating a critical role for the complex during erythrocyte entry (Collins et al., 2009; Richard et al., 2010).

The inability to capture merozoites reliably at every step of invasion, in particular those from the only in vitro culture adapted and most virulent species to infect humans, *P. falciparum*, has been a major impediment to understanding coordination of erythrocyte invasion. Recently, we developed a method to isolate merozoites that retain their invasive capacity (Boyle et al., 2010). Using this approach, we present fluorescence, three-dimensional structured illumination and electron microscopic imaging of *P. falciparum* merozoites caught in the act of erythrocyte entry. Combining these advances in imaging with knockout lines and a panel of specific inhibitors we show that invasion hinges on committed attachment by the merozoite to the erythrocyte surface, which acts as a master switch, triggering all downstream events. Significantly, though, these downstream events continue without apparent further checkpoints, relying instead on the successful orchestration of each event around a formed tight junction—the molecular seal through which invasion proceeds. These data enable us to propose a model for the molecular basis of invasion. Furthermore, the techniques used here provide a simple, widely adoptable approach to functionally evaluate inhibitors of merozoite invasion by wide-field microscopy.

RESULTS

Visualization of *P. falciparum* Merozoite Invasion

Synchronous erythrocyte invasion events by *P. falciparum* merozoites were captured with a recently developed method for the isolation of viable merozoites (Boyle et al., 2010). Investigation of fixed preparations by transmission electron microscopy (TEM) demonstrated that merozoites could be captured and visualized at every step of entry (Figure 1A) and confirmed stages of merozoite invasion that have been defined with other *Plasmodium* species (Aikawa et al., 1978; Bannister et al., 1975; Ladda et al., 1969): nonoriented surface attachment (step 1), apical attachment (2), early tight-junction formation (3, inset), active invasion through the junction into the nascent parasitophorous vacuole (PV) (4–7), sealing of the parasite within the PV (8), and completed entry (9). To correlate these ultrastructural events with molecular events, we undertook immunofluorescence assays (IFAs) of similar preparations using specific antibodies to the rhoptry neck protein PfRON4 (Richard et al., 2010) (Figure S1A available online), an ortholog of the known marker of the tight junction formed during *T. gondii* tachyzoite invasion (Alexander et al., 2005; Lebrun et al., 2005). PfRON4 labeling could be traced from a single point of fluorescence at the merozoite apex on attachment (the rhoptry neck, Figure S1B) through to junction closure at completion of entry (Figure 1B). Notably, midway through invasion, a ring of PfRON4 fluorescence labeling formed (Figure 1B, mid, and Movie S1). After completion of invasion, PfRON4 labeling spread in patches around the expanding PV membrane (PVM), suggesting a loss of structural integrity of the junction at this point (Figure 1B, <10 min). These data establish our ability to visually dissect the mechanics of *P. falciparum* merozoite invasion by microscopy and to identify invasive events, as defined by an intact ring of PfRON4.

A Core Molecular Component of the Merozoite-Erythrocyte Tight Junction: The PfAMA1 and RON Complex Interaction

Having established PfRON4's demarcation of an intact junction, we investigated whether the interaction of the micronemal protein PfAMA1 with the RON complex, which occurs readily in solution (Alexander et al., 2006; Cao et al., 2009; Collins et al., 2009; Richard et al., 2010), was supported by their colocalization at the invasion aperture. In parasites fixed prior to or immediately after egress from E64-treated schizonts (ETS) a significant proportion of PfAMA1 had already been secreted onto the merozoite surface (Figure S2A). Conventional fluorescence imaging of midinvasion merozoites revealed that PfAMA1 labeling localized directly within the plane of the ring of PfRON4 fluorescence (Figure 2A and Figure S2A). A proportion of PfAMA1 was also variably localized to the merozoite surface and unreleased micronemes (Figure 2A and Figure S2A). Three-dimensional structured illumination microscopy (3D SIM) (Schermelleh et al., 2008) demonstrated that this ring of PfAMA1 labeling lies within that of PfRON4 (Figure 2B). To explore this quantitatively, we measured the distance between peak fluorescent intensity of PfRON4 and PfAMA1 labeling, or PfRON4 double labeling (mouse versus rabbit, Figure S1A), across tight junctions ($n \geq 20$) of midinvasion merozoites (Figure 2C). The distance between PfRON4 and PfAMA1 labeling was found to be significantly greater than that of the control measurements (Figure 2D and Figures S2B and S2C; $p < 0.0001$, t test). Since PfAMA1 is known to be on the merozoite surface (Singh et al., 2010), our evidence is consistent with translocation of PfRON4 into the host cell cytosol, as demonstrated for the *T. gondii* ortholog

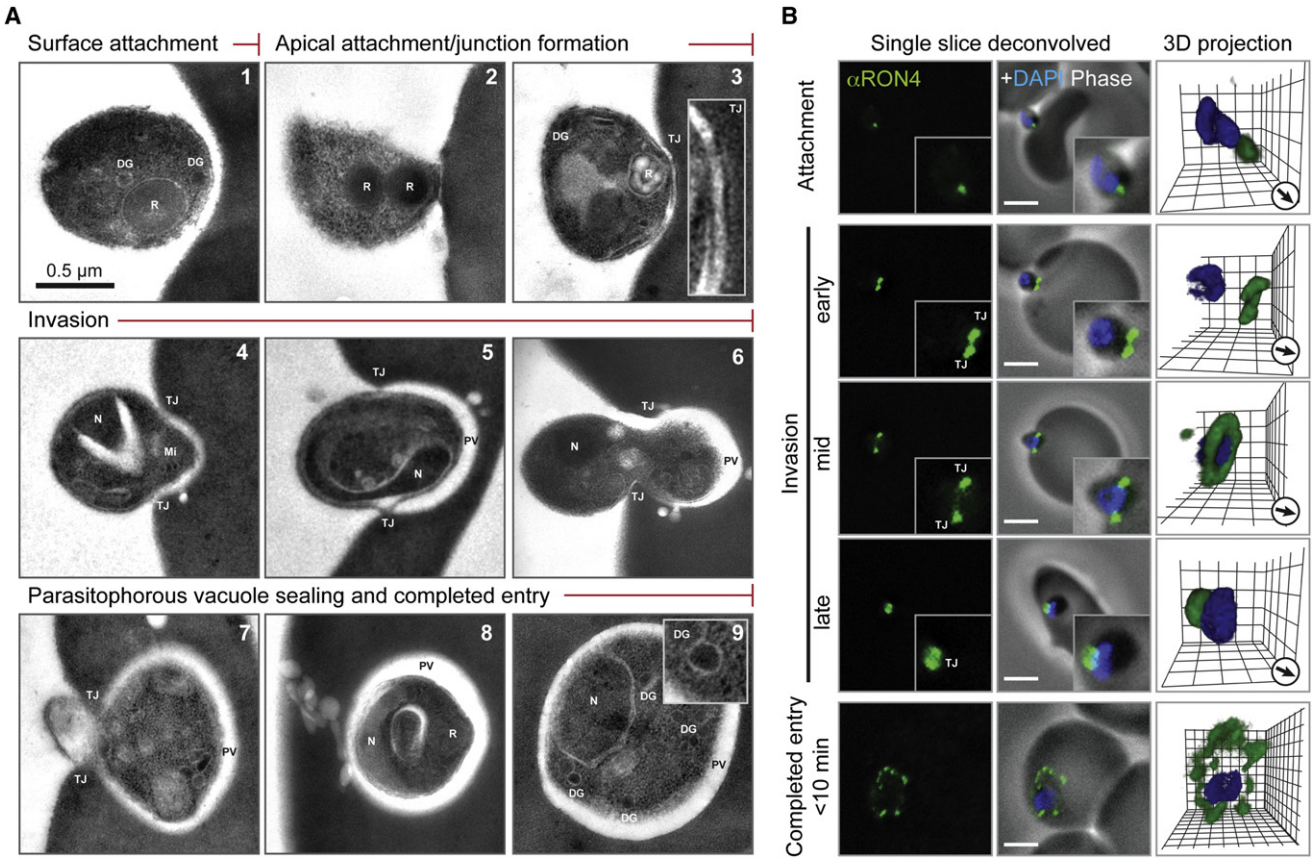

Figure 1. Electron and Immunofluorescence Microscopy of *P. falciparum* Merozoite Invasion

Time courses of invasion by transmission electron microscopy (TEM) (A) and wide-field immunofluoresence assay (IFA) microscopy (B) with deconvolution (single slice or three-dimensional reconstruction) labeled with PfRON4. For TEM numbering, see the main text. The IFA scale bar represents 2.0 μm. In 3D images, gamma settings were altered, and the grid represents 0.5 μm intervals. DG, dense granules; Mi, micronemes; N, nucleus; PV, parasitophorous vacuole; R, rhoptries; TJ, tight junction. See also Figure S1 and Movie S1.

(Besteiro et al., 2009; Straub et al., 2009). This was further suggested by double labeling of invading merozoites with a red blood cell surface marker, glycophorin A (Figures S2D and S2E and Movie S2). For a more decisive localization, we undertook immunoelectron (IEM) microscopy of invading merozoites. PfRON4 immunogold labeling was retained within the rhoptry neck preinvasion but significantly moved, in the majority (Figure 2E), to the cytosolic side of the erythrocyte membrane at the time of attachment (Figure 2F, white arrows). Once inside, labeling could be seen to associate directly with the junction (Figure 2F). These data demonstrate that the well-defined PfAMA1-RON complex interaction occurs predominantly at the merozoite-erthrocyte tight junction and argue strongly in favor of their placement on either side of the erythrocyte boundary.

The Order of Apical Organelle Secretion during Invasion Is a Conserved Feature of Apicomplexan Host-Cell Invasion

We next sought to define key molecular and cellular events that occur at each invasion stage. First, using established markers for key organelles, we investigated the order of apical organelle release during invasion (Bannister et al., 1975). To complement the micronemal protein PfAMA1 (Figure 2A and Figure S2A), we chose *r*hoptry-*a*ssociated *p*rotein 1 (RAP1) as a rhoptry bulb marker (Richard et al., 2009; Schofield et al., 1986) and *r*ing-infected *e*rythrocyte *s*urface *a*ntigen (RESA) as a dense granule marker (Rug et al., 2004).

Preinvasion through to Attachment

Before invasion commencement, and unlike PfAMA1 within micronemes, which was partially released before attachment (Figure S2A), RAP1 clearly remained within the merozoite apex (Figure 3A and Figure S3A, RAP1 early) posterior to the rhoptry neck as defined by PfRON4. RESA was similarly retained within the merozoite body, often at the apical end but frequently basal to rhoptries and micronemes (Figure 3B and Figure S3B, RESA early).

Tight-Junction and Parasitophorous Vacuole Establishment

Midinvasion merozoites revealed that RAP1 labeling had moved to an anterior position beginning immediately adjacent to the junction and tracking the exterior of the merozoite as it entered the invasion pit (Figure 3A and Figure S3A, RAP1 mid). These observations were confirmed by 3D SIM, showing clearly RAP1 transition pre-, mid-, and postinvasion (Figure 3C). This

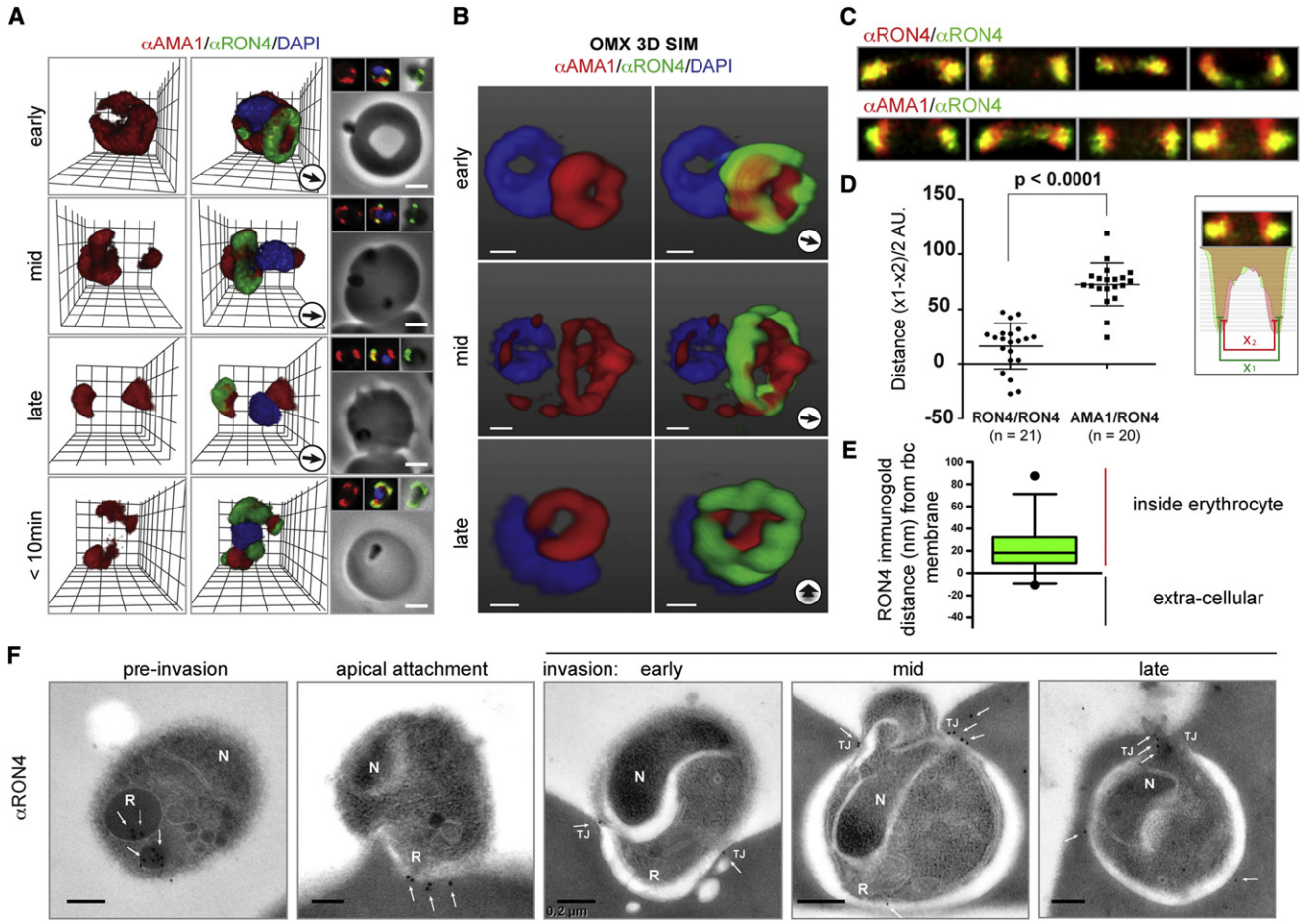

Figure 2. PfAMA1 and PfRON4 Define Core Components of the Merozoite-Erythrocyte Tight Junction

(A) Three-dimensional reconstruction of IFA z stacks showing steps of invasion from attachment through to <10 min after invasion labeled with PfRON4 (green) and PfAMA1 (red). The inset shows a bright-field and single slice with deconvolution. The scale bar represents 2.0 μm.

(B) Three-dimensional structured illumination microscopy (3D SIM) of PfAMA1 and PfRON4 double-labeled merozoites during invasion. The scale bar represents 0.3 μm.

(C) Representative z slices through tight junctions used to measure fluorescence intensity profile across the junction to explore PfAMA1 localization with respect to PfRON4 compared to PfRON4/RON4 double-labeled preparations.

(D) The chart shows the mean distances in arbitrary units between peak intensities across the tight junction (see schematic). Values ±standard deviation comparing PfAMA1 and PfRON4 compared to PfRON4/RON4 double-labeled preparations ($p < 0.0001$, unpaired t test).

(E) Quantification of gold particles either side of the erythrocyte membrane in merozoites with tight junctions immunogold labeled with anti-PfRON4. The chart shows mean and 95% spread.

(F) Representative transmission electron microscopy with immunogold labeling (white arrows) of PfRON4 (the scale bar represents 0.2 μm).

In 3D images gamma settings were altered and grid, where present, represents 0.5 μm intervals. See also Figure S2 and Movies S2.

establishes that release of rhoptry bulb proteins is likely to be concurrent with merozoite passage through the tight junction, with full secretion completed by the time of nascent PV formation. RESA, in contrast, retained its position inside the merozoite, establishing that release of dense granule proteins likely occurs postinvasion (Figure 3B and Figure S3B, RESA mid).

Erythrocyte Sealing and Postinvasion

RAP1 labeling late in invasion showed fluorescence surrounding the entire parasite (Figures 3A and 3C and Figure S3A, RAP1 late). IEM of merozoites at the same stage showed RAP1 immunogold labeling concentrated within the PV space or at the PVM, again consistent with release of rhoptry bulb proteins at this time (Figure 3D, white arrows). For RESA, localization became markedly more peripheral and evenly distributed around the merozoite immediately after invasion (Figure 3B and Figure S3B, RESA late), supporting the notion that dense granules are released after invasion at the merozoite plasma membrane, as previously suggested by studies with simian malaria parasites (Bannister et al., 1975; Culvenor et al., 1991; Torii et al., 1989). TEM confirmed that dense granules remain intact at this point (Figures 1A and 3E). Closure of the tight junction and sealing of the PVM occurs within 10 min of invasion (Figure 1). At this time, RAP1 labeling revealed prominent extensions of the PV into the erythrocyte cytosol (Figure 3A and Figure S3A, RAP1 < 10 min), as confirmed by IEM (Figure 3F). This pattern of labeling would strongly support the localization of RAP1 to structures previously

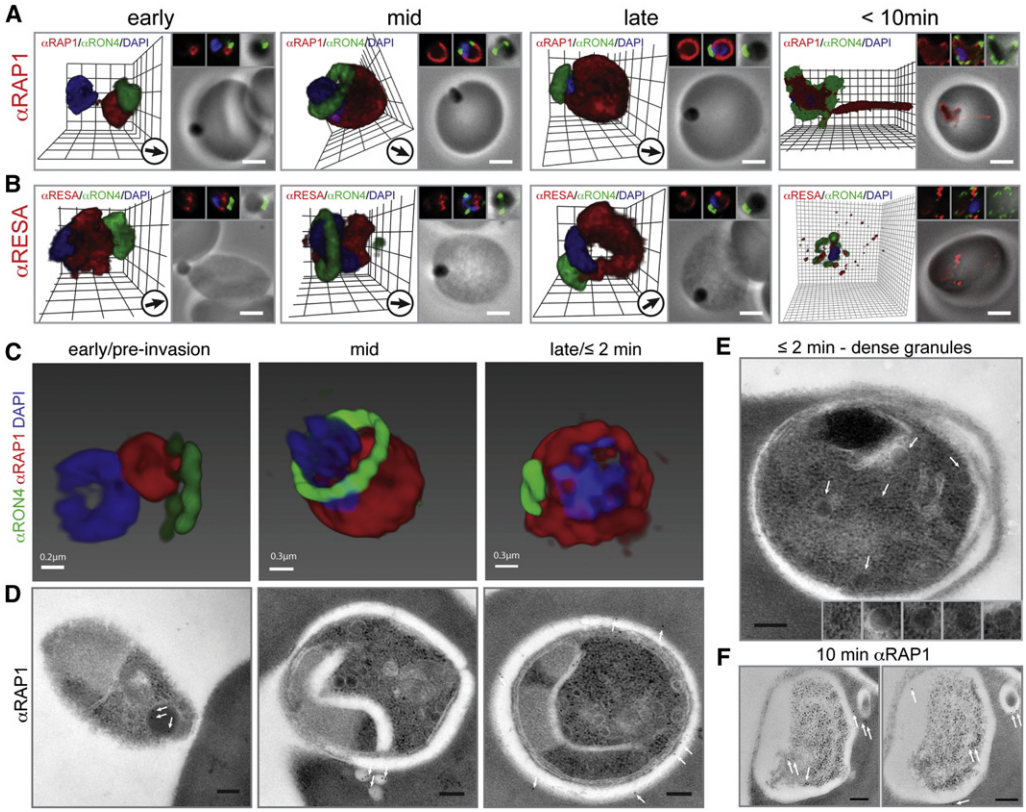

Figure 3. Stepwise Secretion of Apical-Organelle Resident Proteins from Rhoptries and Dense Granules, during Invasion

(A and B) Three-dimensional reconstruction of IFA z stacks showing steps of invasion from attachment (early), through mid and late invasion, to <10 min after invasion labeled with resident proteins of the rhoptry bulb (RAP1) (A) and dense granules (RESA) (B). Insets show bright-field and single slice deconvolution. The scale bar represents 2.0 μm. In 3D images, gamma settings were altered, and the grid represents 0.5 μm intervals.

(C) 3D SIM time course of invasion labeled with anti-RAP1.

(D) Electron microscopy with immunogold labeling of RAP1 (white arrows). The scale bar represents 0.2 μm.

(E) Electron microscopy of merozoite after invasion showing intact dense granules (white arrows and insets). The scale bar represents 0.2 μm.

(F) Serial sections of electron microscopy with immunogold labeling of RAP1 10 min after invasion (white arrows). The scale bar represents 0.2 μm.

See also Figure S3.

reported by EM with simian malaria parasites (Bannister et al., 1975; Torii et al., 1989). Signs of RESA translocation via dense granule release into the erythrocyte cytosol (absent in ≤2 min samples, data not shown) were already apparent as punctate areas of fluorescence (Figure 3B and Figure S3B, RESA < 10 min).

Our ability to time invasion and postinvasion events to the first few minutes before and after entry combined with imaging of microneme (Figure 2), rhoptry, and dense granule (Figures 1 and 3) resident proteins strongly supports a general order of organelle secretion—microneme, rhoptry, and finally dense granule contents—as a conserved feature of apicomplexan host-cell invasion (Carruthers and Sibley, 1997). Furthermore, they establish that export of proteins into the erythrocyte cytosol is initiated rapidly (within 10 min) after merozoite entry is completed.

The Tight Junction Acts as the Nexus for Motor Engagement and Merozoite Surface Protein Release

We next explored the timing of two key molecular events of invasion: surface protein shedding (Blackman et al., 1990) and actomyosin motor function (Miller et al., 1979). TEM has demonstrated the loss of a fibrillar surface coat of unknown molecular nature with merozoite progression through the tight junction (Aikawa et al., 1978; Bannister et al., 1975). We focused on the dominant surface protein MSP1, using antibodies to its processed ectodomain that is released during erythrocyte entry (Blackman et al., 1990; Boyle et al., 2010). To explore the site of shedding, we also investigated the localization of the microneme protein PfSUB2, the sheddase responsible for MSP1 release (Harris et al., 2005b), following a published strategy to epitope tag the endogenous locus (as per Harris et al. [2005b] and Figure S4B). Finally, as a marker for the engaged actomyosin motor, we used antibodies to *Plasmodium* actin (F.A. and J.B., unpublished data), which show strong specificity for malarial compared to erythrocyte actin (Figure S4D).

Preinvasion through to Attachment

Before commencement of invasion, no loss of MSP1 labeling was apparent (Figure 4A and Figure S4A, MSP1 early) (Boyle et al., 2010). However, even in parasites at early stages of invasion, the majority of PfSUB2 had reached the posterior pole of the merozoite (Figure 4B and Figure S4C, PfSUB2 early) with a minority remaining apical, presumably within unsecreted

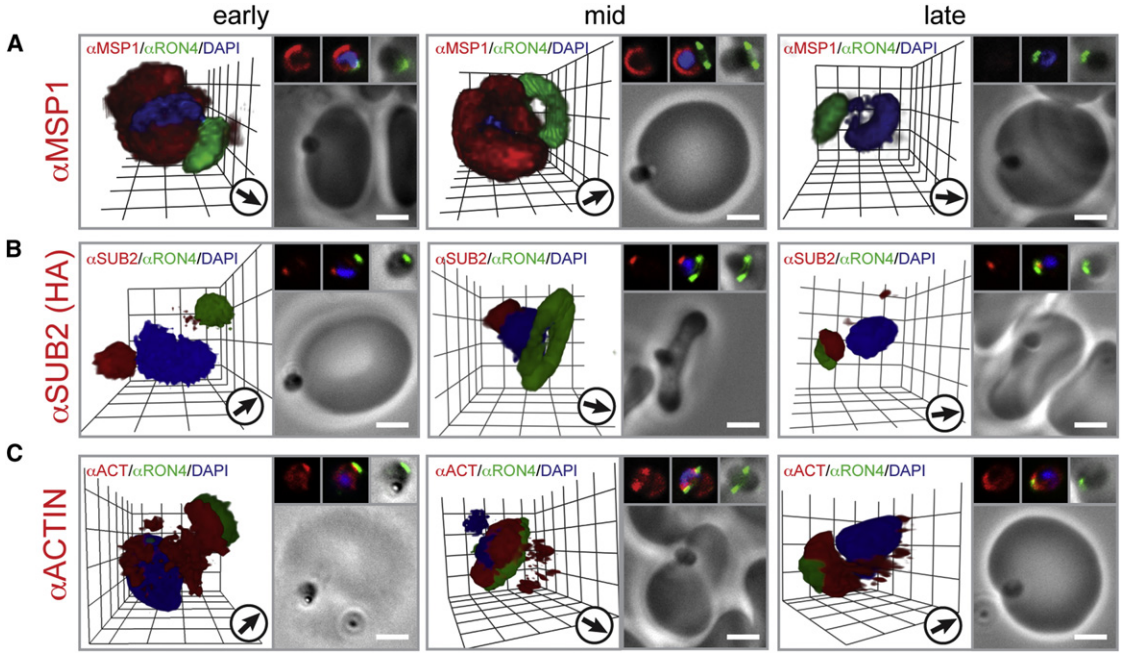

Figure 4. Coordination of Surface Protein Shedding and Actomyosin Motor Engagement during Invasion

Three-dimensional reconstruction of IFA z stacks showing steps of invasion from attachment (early), through mid and late invasion labeled with markers for the merozoite surface (MSP1) (A), the MSP1 sheddase (PfSUB2—tagged with an endogenous HA epitope) (B), and parasite actin (C). Insets show bright-field and single slice deconvolution. The scale bar represents 2.0 μm. In 3D images, gamma settings were altered, and the grid represents 0.5 μm intervals. See also Figure S4 and Movie S4.

micronemes, in some parasites (data not shown). The distribution of actin within the merozoite was concentrated at the parasite apex, with diffuse labeling elsewhere in the cytoplasm (Figure 4C and Figure S4E, Actin early).

Tight-Junction and Parasitophorous Vacuole Establishment

Loss of MSP1 tracked the exterior of invading merozoites concurrent with different stages of passage through the tight junction (Figure 4A and Figure S4A, MSP1 mid) (Boyle et al., 2010) resolving at the molecular level, descriptive observations of surface coat removal by TEM (Aikawa et al., 1978; Bannister et al., 1975). Although not colocalized in the same parasite, the lack of contiguity between shed MSP1 and PfSUB2 sheddase, each in comparison with PfRON4 (Figure 4B and Figure S4C, PfSUB2 mid), suggests that MSP1 may be processed by PfSUB2 early in invasion but shed only during passage through the junction. Midway through invasion, a distinct ring of anti-Actin fluorescence could be detected, concentrated at the tight junction (Figure 4C, Figures S4E and S4F, and Movie S4, Actin mid). Since active invasion requires engagement of the parasite actomyosin motor (Baum et al., 2006a), in particular the polymerization of actin (Miller et al., 1979), a high concentration of actin filaments would be predicted to occur at the junction itself.

Erythrocyte Sealing and Postinvasion

In the latter stages of invasion, the complete absence of MSP1 labeling demonstrates that total surface processing (of MSP1 at least) occurred with completion of invasion (Figure 4A and Figure S4A, MSP1 late) (Boyle et al., 2010). PfSUB2 remained at the posterior pole (Figure 4B and Figure S4C, SUB2 late). At this time, the concentration of actin labeling was, as expected, at the rear of the invaded merozoite (Figure 4C and Figure S4E, Actin late).

Combined, these data suggest that the tight junction acts as the nexus around which the traction force for invasion, as determined by actin-dependent engagement of the gliding motor, and shedding of merozoite surface proteins occurs. However, discontinuity between the junction cleavage of MSP1 and posterior localization of PfSUB2 suggests that proteolytic cleavage and actual shedding may not occur at the same sites.

Commitment to Invasion Is Mediated by Merozoite Invasion Adhesins and Stabilized by Tight-Junction Formation

Having described core cellular and molecular steps of invasion, we set out to explore the hierarchy of their coordination, beginning with erythrocyte recognition. Merozoites are likely primed for invasion at egress, in particular through the release of invasion adhesins prior to or on release from the infected erythrocyte (Singh et al., 2010). While the precise mechanism for erythrocyte recognition is unknown, two adhesin families likely mediate merozoite commitment to invasion of a target red cell: the *e*rythrocyte-*b*inding-*l*ike antigens/*d*uffy-*b*inding-*l*ike proteins (EBL/DBL) and *r*eticulocyte-binding protein *h*omologues (PfRh) (Cowman and Crabb, 2006; Singh et al., 2005). These in turn mediate invasion through alternative pathways, variously dependent on sialic-acid residues of erythrocyte surface receptors (Baum et al., 2005; Duraisingh et al., 2003b; Stubbs et al., 2005). Attempts to explore the distribution of different EBL and

PfRh proteins by fluorescence microscopy (using multiple mouse and rabbit sera) were inconclusive, showing poor resolution with the fixation methods used (data not shown).

As an alternative, quantitative approach to explore the role of PfRh and EBL invasion adhesions, we used gene knockouts for PfRh4 (Stubbs et al., 2005) and EBA175 (Duraisingh et al., 2003a) on the W2mef parasite background—two proteins that carry out functionally complementary roles in invasion (Stubbs et al., 2005). In the PfRh4KO line, absence of PfRh4 makes invasion critically dependent on usage of erythrocyte sialic-acid residues, likely through EBA175-receptor binding (Stubbs et al., 2005). This pathway can be blocked by pretreatment of erythrocytes with neuraminidase (Nm), which removes sialic-acid residues from erythrocyte receptors. In the EBA175KO line (unlike the parent line) upregulation of PfRh4 permits sialic acid-independent invasion via this parasite adhesin (Stubbs et al., 2005). Merozoite attachment assays, in which the degree of attachment (distinct from invasion) can be measured (Figures S5A and S5B), with PfRh4KO parasites demonstrated that the percentage of surface-bound merozoites to Nm-treated erythrocytes was significantly reduced compared to untreated erythrocyte controls using the same knockout line (Figure 5A, mean = 30% ± 7% SEM). Since EBA175 is the dominant invasion ligand, and likely determinant of sialic-acid dependent invasion in this parasite strain (Stubbs et al., 2005), this suggests a role for EBA175 in directly mediating attachment. A reduction compared to untreated controls was not seen with the attachment of EBA175KO merozoites to Nm-treated cells (Figure 5A, mean = 97% ± 2% SEM). Since PfRh4 is the determinant of sialic acid-independent invasion in the EBA175KO parasite (Stubbs et al., 2005), cross-comparison between knockout lines would also support PfRh4 as having a direct role in mediating surface attachment to the erythrocyte.

Attachment assays incorporated a proportion of merozoites associated with erythrocytes under all conditions tested (see the Experimental Procedures). IFA inspection was undertaken to explore the molecular nature of merozoites found attached to Nm-treated erythrocytes. Labeling with PfRh4KO revealed that most lacked an established tight junction (as indicated by a ring of PfRON4 labeling) compared to those found in untreated controls (Figure 5B, inset shows "established tight junction" definition). As such, these were, in the majority, breakthrough from the wash steps rather than actively invading parasites. Together, these data support a direct role for PfRh4 and probably EBA175 in mediating committed attachment of merozoites to erythrocytes upstream of tight-junction formation. We next explored how other events behave with respect to attachment. Merozoite attachment assays in the presence of a 20 residue inhibitory peptide (R1) (Harris et al., 2005a), which blocks formation of the PfAMA1-RON complex (Richard et al., 2010), showed~50% reduction in the proportion of bound merozoites to untreated controls (Figure 5A, mean = 44% ± 15% SEM). As with Nm-treated PfRh4KO, few of the R1-treated merozoites found associated with erythrocytes demonstrated tight-junction establishment (Figure 5B, mean = 8% ± 6% SEM) as predicted (Richard et al., 2010). However, presence of cytochalasin D (cytoD), an inhibitor of actomyosin motor function (Miller et al., 1979), or phenylmethylsulfonyl fluoride (PMSF), a serine protease inhibitor that blocks processing of the surface

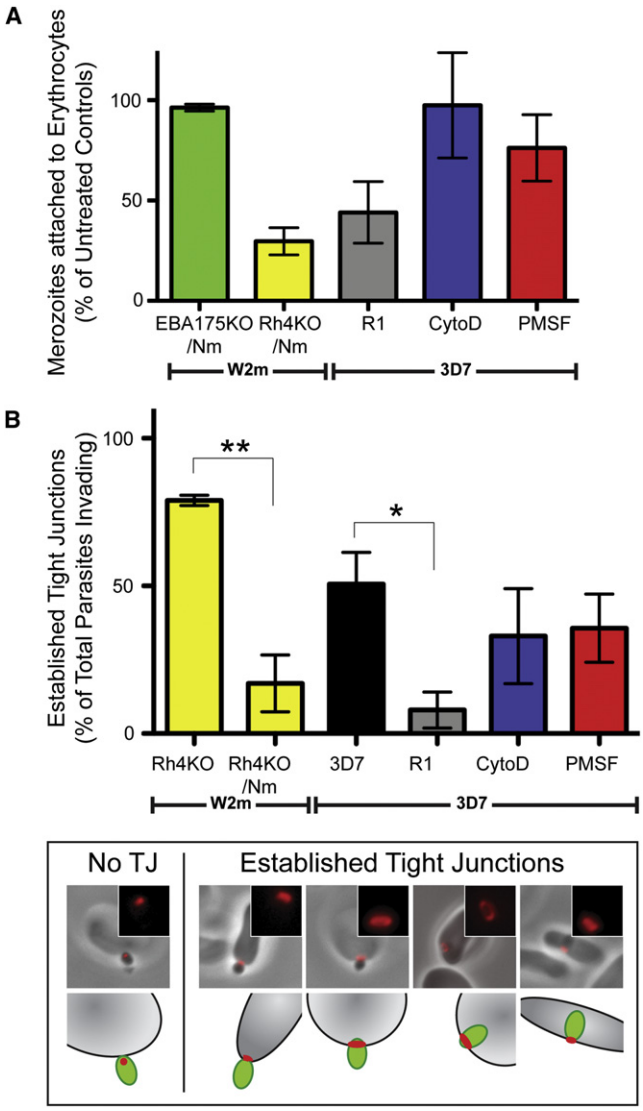

Figure 5. Merozoite Attachment Mediated by Apical Adhesins Is the First Step in Committed Invasion

(A) Number of attached merozoites, expressed as a percentage of untreated controls for two knockout parasite lines, PfRh4KO and EBA175KO, invading neuraminidase (Nm)-treated erythrocytes and three inhibitors of invasion: 1 mg/ml R1 inhibitory peptide, 1 μM cytochalasin D (CytoD), and 1 mM phenylmethanesulfonyl fluoride (PMSF).

(B) Number of identifiable established PfRON4 tight junctions (defined by scheme—see inset) expressed as a percentage of the total number of merozoites seen attached to erythrocytes.

All chart values displayed represent mean ± SEM of three independent assays repeated in triplicate. *$p < 0.05$, **$p < 0.01$ (unpaired t test). See also Figure S5.

proteins PfAMA1 and MSP1 (Howell et al., 2003), gave no reduction in the number of attached merozoites compared to untreated controls (Figure 5A). Furthermore, neither treatment, despite their inhibitory effects on invasion (Boyle et al., 2010; Miller et al., 1979) (Figure S5C), significantly reduced tight-junction formation as marked by PfRON4 labeling (Figure 5B). This demonstrates that a hierarchy exists in the molecular events of invasion. PfRh/EBL proteins likely mediate committed

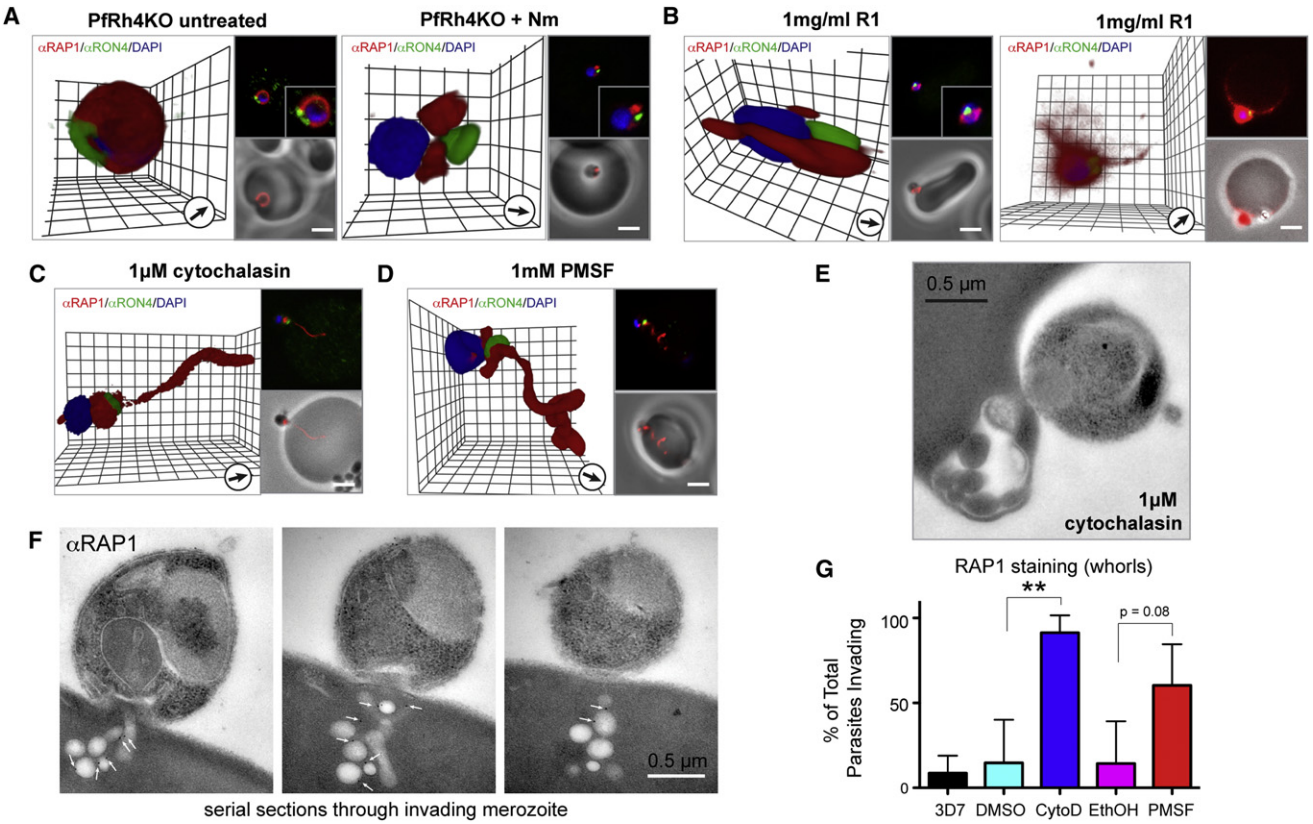

Figure 6. Coordination between Invasion Events after Committed Merozoite Attachment

(A–D) Three-dimensional reconstruction of deconvolved z stacks, labeled with anti-PfRON4 and anti-RAP1, showing examples of PfRh4KO merozoite invasion into untreated versus Nm-treated erythrocytes (A), Parasite invasion in the presence of R1 inhibitory peptide (B), 1 μM CytoD (C), and 1 mM PMSF (D). Insets shows bright-field and single slice with deconvolution. The scale bars represent 2.0 μm. In 3D images gamma settings were altered and grid represents 0.5 μm intervals.

(E) Electron microscopy of 1 μM CytoD-treated merozoite showing aberrant rhoptry release.

(F) Serial section electron microscopy with immunogold labeling of RAP1 showing colocalization of RAP1 with rhoptry-derived membrane into erythrocyte cytosol during an untreated merozoite invasion event.

(G) Number of identifiable aberrant rhoptry whorls seen, as demarked by RAP1 labeling, as a percentage of the total number of merozoites seen attached to erythrocytes with CytoD and PMSF treatment. Chart values displayed represent mean ± SEM of three independent assays repeated in triplicate. **$p < 0.01$ (one-tailed t test).

See also Figure S6.

attachment to the erythrocyte, committing the merozoite to host cell invasion, which may then be stabilized by tight-junction formation. Motor activity and proteolytic shedding of surface proteins play no role in either process and therefore function downstream.

Coordination of Downstream Events of Invasion Follows Committed Merozoite Attachment

To differentiate the hierarchy of downstream events from committed attachment, we explored the timing of rhoptry release. This cellular event can be trigged in the absence of erythrocytes by incubating merozoites with soluble invasion receptors (Singh et al., 2010), suggesting a link between committed attachment and rhoptry release. PfRh4KO parasites in the process of invasion into untreated erythrocytes exhibited normal RAP1 release (Figure 6A and Figure S6A). However, those found associated with Nm-treated erythrocytes showed RAP1 labeling retained in the merozoite apex anterior to PfRON4 labeling (Figure 6A and Figure S6B). This is consistent with rhoptry release being dependent on PfRh/EBL receptor binding (Singh et al., 2010).

Merozoite invasion in the presence of the R1 peptide also demonstrated rhoptry bulb release. However, unlike normal invasion, RAP1 was released aberrantly onto the merozoite or erythrocyte surface and not into the host cell (Figure 6B) (mean = 48.7% ± 7.33% SEM, more merozoites showed aberrant surface release compared to untreated controls, $p < 0.05$, paired t test). This is akin to that previously described as abortive merozoite invasion (Sterkers et al., 2007). Electron microscopic inspection of R1-treated parasites demonstrated an increased number of merozoites with aberrant apical extrusions, consistent with anomalous and premature rhoptry release (Figure S6C). This demonstrates that even in the absence of tight-junction establishment (or with R1-dependent mimicking of the interaction between PfAMA1 and the RON complex), full rhoptry secretion proceeds without coordination. This suggests that while

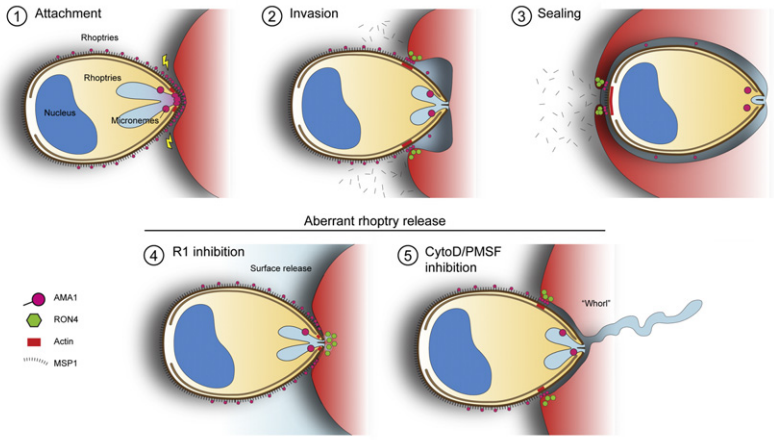

Figure 7. Schematic Model for *Plasmodium falciparum* Merozoite Invasion of the Erythrocyte

See the main text for details. After a low-affinity attachment, merozoite reorientates to its apical pole, where committed attachment initiates the master signal (yellow lightning bolt) for all downstream events (1). Coordinated entry into the erythrocyte is orchestrated around the established tight junction and includes rhoptry secretion, generation of nascent PV and PVM, activation of actomyosin motor, and shedding of the merozoite surface coat (2) Sealing of the invaded merozoite ends the invasion process followed rapidly by development of the early trophozoite and erythrocyte remodelling (not shown) (3). Inhibition of invasion by the R1 peptide (blocks PfAMA1/RON complex interaction) (4) or cytochalasin (disrupts motility) or PMSF (disrupts surface coat shedding) (5) leads to aberrant rhoptry release.

tight-junction formation, or the signal that follows AMA1-RON complex interaction, may play a role in stabilizing attachment, it is triggered downstream of the attachment step and the signal attachment gives for rhoptry release.

Rhoptry bulb release could also be seen to occur in parasites treated with either cytoD or PMSF. However, unlike normal capping of the invading merozoite (Figure 6A), or aberrant surface release as seen in the presence of R1 (Figure 6B), RAP1 was secreted into the host cell as a whorl-like structure spread through the erythrocyte cytosol (Figures 6C and 6D). Such whorls could be seen by electron microscopic inspection of cytochalasin-treated merozoite preparations (Figure 6E). Similar structures have been seen by electron microscopy with uninhibited merozoite invasion (Bannister et al., 1986; Miller et al., 1979). Indeed, 3D SIM (Figure S6D) or electron microscopy (Figure 6F) identified several such events, demonstrating passage of rhoptry contents through the eye of the tight junction (Figure S6D) and, via immunogold labeling, localizing RAP1 to vesicular structures inside the erythrocyte (Figure 6F). Quantification of the number of rhoptry-derived whorls seen with invading merozoites in treated versus untreated preparations (as labeled with RAP1) show that such structures are, however, less frequent in untreated invasion events (Figure 6G, untreated = 9%, cytoD = 91%, PMSF = 60%).

Combined with data from PfRh4KO merozoite attachment of Nm-treated erythrocytes, these data strongly suggest that rhoptry release, correct tight-junction formation, actomyosin activation, and surface protein shedding are all triggered after committed attachment—an event likely initiated by EBL/PfRh proteins. Since each proceeds irrespective of the other, these data demonstrate that initiation of the mechanics of invasion likely requires only a singular master initiation switch (attachment), with the process then proceeding without checkpoints to full merozoite entry.

DISCUSSION

Our ability to image, in detail, key molecular and cellular events during *P. falciparum* merozoite invasion provides a unique window into the mechanics that underlie penetration of this deadly parasite into the human erythrocyte. Significantly, our findings indicate that merozoite attachment to the erythrocyte is likely to be the master switch triggering all downstream events, which, once initiated, results in the unstoppable progression of invasion: secretion of rhoptry neck followed by rhoptry bulb, tight-junction establishment, surface shedding, and motor activation. Our evidence for lack of coordination between downstream events, combined with video microscopy observations of R1-treated merozoites actively pulling on the erythrocyte surface (Richard et al., 2010; Treeck et al., 2009) (i.e., retaining active motility in the absence of a tight junction), supports the notion that these events proceed without further checkpoints. In addition, we demonstrate that successful interaction between PfAMA1 and the RON complex, across the two faces of the merozoite-erythrocyte tight junction, defines a molecular seal through which the rhoptry bulb contents passes. Importantly, the tight junction appears to act as a nexus, orchestrating each of these key events associated with invasion.

Combining our data with those from previous studies allows us to propose a stepwise model for establishing asexual blood stage infection (Figure 7). Merozoites, preinvasion or at the moment of egress, exist in an activated state, with their exposure to extracellular ionic conditions triggering microneme release onto the parasite surface, an event probably signaled by release of intracellular calcium stores (Singh et al., 2010; Treeck et al., 2009). On encountering an erythrocyte, the low-affinity interaction between the merozoite surface and erythrocyte (likely mediated via surface MSPs) is translated into a step of irreversible or committed attachment, possibly concurrent with merozoite reorientation to its apex (Dvorak et al., 1975; Gilson and Crabb, 2009). Evidence presented here and from knockout studies with other EBL proteins (Singh et al., 2005) would support committed attachment as being mediated by EBL/PfRh proteins (step 1). This step is the master switch that triggers all downstream events.

The internal structure of the rhoptries then facilitates the ordering of two key events. The rhoptry neck secretes its contents first, translocating PfRON4, possibly with other members of the RON complex, to the cytosolic side of the erythrocyte plasma membrane (step 2). This complex, likely through RON2 (Besteiro et al., 2009), then provides the anchor for PfAMA1 already on the parasite surface (released via micronemal

discharge at egress). The meeting of PfAMA1 and the RON complex defines the molecular seal of the tight junction, which then channels the rhoptry bulb contents into the erythrocyte. This release is an unstoppable consequence of triggering rhoptry discharge. As such, even when junction formation or merozoite progression is inhibited (such as via cytochalasin or PMSF treatment), rhoptry contents are fully released either aberrantly onto the merozoite or erythrocyte surface (e.g., after R1 treatment) or as continuous tubular whorls into the erythrocyte cytosol (cytochalasin or PMSF) (4 and 5). The possibility that the secretion of rhoptry-derived lipid material ahead of the invading parasite is a transient feature of all native invasion, akin to the evacuoles described in *T. gondii* host cell invasion (Hakansson et al., 2001), cannot be excluded. However, the nature of evacuoles as discrete vesicles would suggest they are not homologous to the tubular structures seen here. The signals to initiate motility are also likely given concurrently with rhoptry release, with polymerization of actin occurring in situ at the tight junction. Surface shedding of merozoite MSPs also occurs at this site, however, it is possible that proteolytic cleavage of proteins has already occurred. The end of invasion is brought about by sealing of the erythrocyte membrane (step 3). Finally, once sealed, and within a few minutes of invasion, dense granules are secreted (not shown), initiating the stages of protein export into the erythrocyte and commencing the dramatic process of host-cell remodeling.

Our work raises several key questions. Foremost, what is the nature of the master signal that arises at committed attachment? Recent data suggest that it likely involves signaling cascades initiated through the cytoplasmic tails of surface adhesins (Dvorin et al., 2010; Leykauf et al., 2010; Treeck et al., 2009). Additionally, how is PfRON4 translocated across the erythrocyte membrane? Loss of integrity in the erythrocyte membrane may not be necessary for its insertion into the host cell but might instead proceed through a fusion of merozoite and erythrocyte derived membranes within the invasion pit (Aikawa et al., 1978; Bannister et al., 1975). Indeed, abundant lipid material seen with invading *P. knowlesi* merozoites has been observed at this site (Bannister et al., 1986). The nature of the interaction between parasite and erythrocyte membranes raises a further question about the molecular nature of the tight junction and its ability to selectively permit transit of certain erythrocyte proteins and lipids through its structure (Dluzewski et al., 1989; Lauer et al., 2000).

The ability to dissect in detail the spatial and temporal localization of key molecular and cellular events during *P. falciparum* merozoite invasion provides a powerful platform to explore strategies to block the process. The predominance of blood stage antigens specifically, and invasion adhesins in general, in current vaccine strategies can now be explored in detail as to the nature of the inhibitory effects seen. This allows testing of long standing hypotheses about how antibodies against malaria antigens actually protect the host from infection. Furthermore, there is now a concrete methodological foundation to test assertions about the nature and function of the ever-increasing number of antigens implicated in the invasion process. This provides a complementary arm to genetic strategies that explore parasite protein function, in particular for those essential antigens that are unable to be knocked out or genetically tagged.

EXPERIMENTAL PROCEDURES

Additional detailed methods are presented in the Supplemental Experimental Procedures available online. All chemicals were from Sigma unless otherwise stated.

Merozoite Preparation and Invasion Imaging

Merozoites were isolated as described (Boyle et al., 2010) by passing 7–8 hr 10 μM E64-treated schizonts (ETSs) through a 1.2 μm, 32 mm syringe filter (Sartorius Stedim Biotech, France). Filtered merozoites were added to uninfected erythrocytes and processed for invasion or growth inhibition. Invading merozoites were captured after 2 or 10 min incubation with erythrocytes, shaking at 37°C. Samples were then processed for IFA, EM, or 3D SIM (see the Supplemental Experimental Procedures).

Merozoite Attachment Assays

Inhibitory compounds were added to filtered 3D7 merozoites prepared as described above at 1 mg/ml R1 peptide (diluted in culture medium), 1 μM cytochalasin D (DMSO) and 1 mM PMSF (Ethanol). After 2 to 10 min incubation, uninfected erythrocytes were added and invasion allowed to proceed for 2 min before fixation. Control assays were performed with dilutions of 1/10000 DMSO for cytochalasin, 1/500 ethanol for PMSF, or media only for R1. After fixation and washing, merozoite-bound erythrocytes were labeled with DAPI. Imaging used the Mosaic function of Axiovision software, scoring three biological replicates of approximately 2000 erythrocytes along with bound merozoites per condition.

Image Processing

Deconvolved Z stacks were reconstructed in 3D, with interpolation, using Imaris version 6.4.2 or 7.0.0 (Bitplane Scientific). For clarity of display, gamma settings were altered on 3D reconstructions after deconvolution; however, no comparisons of labeling levels were made from such altered images. General image handling was undertaken with either Image J or Adobe Photoshop CS4. Final images were assembled in Adobe Illustrator CS4 for figure generation. For junction measurements, invasion events occurring along the x-y plane (tight-junction ring along the z axis) were imaged. WIth only RON4-Alexa488 channel data, the z slice of greatest junction diameter was chosen, and an intensity profile was taken in the x-y plane, along a line parallel to the edge of the junction, with the Imaris MeasurmentPro module. Peak fluorescence was determined as the midpoint of the full-width of signal at three-quarter maximum intensity. Final distance was calculated as [distance green(x_1) – distance red (x_2)]/2. Distances were calculated from raw data files as three independent replicates by two observers (see Figure S2). Statistics were calculated with an unpaired t test in Prism 5.0 (Graph Pad Software) software.

SUPPLEMENTAL INFORMATION

Supplemental Information includes Supplemental Experimental Procedures, six figures, and three movies and can be found with this article online at doi:10.1016/j.chom.2010.12.003.

ACKNOWLEDGMENTS

We wish to thank Liz Zuccala for experimental help, Freya Fowkes for advice with statistical analysis, Buzz Baum, Waihong Tham, and Justin Boddey for critical reading of the manuscript, and David Conway, Kevin Tetteh, and Robin Anders for antibodies against MSP1 block 2 and RESA. Human erythrocytes were kindly provided by the Red Cross Blood Bank (Melbourne). This work was supported by the National Health and Medical Research Council (NHMRC) of Australia (Project Grant 637340 J.B. and S.A.R.). D.T.R. is supported through a Pratt Foundation postgraduate scholarship from the University of Melbourne; D.R. is supported by a Canadian Institutes of Health Research postdoctoral fellowship; M.J.B. is supported by an Australian Postgraduate Award and Medicine, Dentistry and Health Sciences Top-Up Scholarship through the University of Melbourne; L.T. is supported by a Chancellor's Postdoctoral Fellowship from the University of Technology Sydney; C.B.W. is supported by a Senior Research Fellowship from the NHMRC; S.A.R. and J.G.B. are supported by Australian Research Council

(ARC) Future Fellowships (FT0990350 and FT0992317 respectively); A.F.C. is a Howard Hughes International Scholar and an Australia Fellow of the NHMRC; and J.B. is supported through an NHMRC Career Development Award I (516763) and ARC Future Fellowship (FT100100112).

Received: July 16, 2010
Revised: October 1, 2010
Accepted: December 10, 2010
Published: January 19, 2011

REFERENCES

Aikawa, M., Miller, L.H., Johnson, J., and Rabbege, J. (1978). Erythrocyte entry by malarial parasites. A moving junction between erythrocyte and parasite. J. Cell Biol. *77*, 72–82.

Aikawa, M., Miller, L.H., Rabbege, J.R., and Epstein, N. (1981). Freeze-fracture study on the erythrocyte membrane during malarial parasite invasion. J. Cell Biol. *91*, 55–62.

Alexander, D.L., Mital, J., Ward, G.E., Bradley, P., and Boothroyd, J.C. (2005). Identification of the Moving Junction Complex of Toxoplasma gondii: A Collaboration between Distinct Secretory Organelles. PLoS Pathog. *1*, e17.

Alexander, D.L., Arastu-Kapur, S., Dubremetz, J.F., and Boothroyd, J.C. (2006). Plasmodium falciparum AMA1 binds a rhoptry neck protein homologous to TgRON4, a component of the moving junction in Toxoplasma gondii. Eukaryot. Cell *5*, 1169–1173.

Bannister, L.H., Butcher, G.A., Dennis, E.D., and Mitchell, G.H. (1975). Structure and invasive behaviour of Plasmodium knowlesi merozoites in vitro. Parasitology *71*, 483–491.

Bannister, L.H., Mitchell, G.H., Butcher, G.A., and Dennis, E.D. (1986). Lamellar membranes associated with rhoptries in erythrocytic merozoites of Plasmodium knowlesi: a clue to the mechanism of invasion. Parasitology *92*, 291–303.

Baum, J., Maier, A.G., Good, R.T., Simpson, K.M., and Cowman, A.F. (2005). Invasion by P. falciparum Merozoites Suggests a Hierarchy of Molecular Interactions. PLoS Pathog. *1*, e37.

Baum, J., Papenfuss, A.T., Baum, B., Speed, T.P., and Cowman, A.F. (2006a). Regulation of apicomplexan actin-based motility. Nat. Rev. Microbiol. *4*, 621–628.

Baum, J., Richard, D., Healer, J., Rug, M., Krnajski, Z., Gilberger, T.W., Green, J.L., Holder, A.A., and Cowman, A.F. (2006b). A conserved molecular motor drives cell invasion and gliding motility across malaria lifecycle stages and other apicomplexan parasites. J. Biol. Chem. *281*, 5197–5208.

Besteiro, S., Michelin, A., Poncet, J., Dubremetz, J.F., and Lebrun, M. (2009). Export of a Toxoplasma gondii rhoptry neck protein complex at the host cell membrane to form the moving junction during invasion. PLoS Pathog. *5*, e1000309.

Blackman, M.J., Heidrich, H.G., Donachie, S., McBride, J.S., and Holder, A.A. (1990). A single fragment of a malaria merozoite surface protein remains on the parasite during red cell invasion and is the target of invasion-inhibiting antibodies. J. Exp. Med. *172*, 379–382.

Boyle, M.J., Wilson, D.W., Richards, J.S., Riglar, D.T., Tetteh, K.K., Conway, D.J., Ralph, S.A., Baum, J., and Beeson, J.G. (2010). Isolation of viable Plasmodium falciparum merozoites to define erythrocyte invasion events and advance vaccine and drug development. Proc. Natl. Acad. Sci. USA *107*, 14378–14383.

Cao, J., Kaneko, O., Thongkukiatkul, A., Tachibana, M., Otsuki, H., Gao, Q., Tsuboi, T., and Torii, M. (2009). Rhoptry neck protein RON2 forms a complex with microneme protein AMA1 in Plasmodium falciparum merozoites. Parasitol. Int. *58*, 29–35.

Carruthers, V.B., and Sibley, L.D. (1997). Sequential protein secretion from three distinct organelles of Toxoplasma gondii accompanies invasion of human fibroblasts. Eur. J. Cell Biol. *73*, 114–123.

Collins, C.R., Withers-Martinez, C., Hackett, F., and Blackman, M.J. (2009). An inhibitory antibody blocks interactions between components of the malarial invasion machinery. PLoS Pathog. *5*, e1000273.

Cowman, A.F., and Crabb, B.S. (2006). Invasion of human red blood cells by malaria parasites. Cell *124*, 755–766.

Culvenor, J.G., Day, K.P., and Anders, R.F. (1991). Plasmodium falciparum ring-infected erythrocyte surface antigen is released from merozoite dense granules after erythrocyte invasion. Infect. Immun. *59*, 1183–1187.

Dluzewski, A.R., Fryer, P.R., Griffiths, S., Wilson, R.J., and Gratzer, W.B. (1989). Red cell membrane protein distribution during malarial invasion. J. Cell Sci. *92*, 691–699.

Doolan, D.L., Dobano, C., and Baird, J.K. (2009). Acquired immunity to malaria. Clin. Microbiol. Rev. *22*, 13–36.

Duraisingh, M.T., Maier, A.G., Triglia, T., and Cowman, A.F. (2003a). Erythrocyte-binding antigen 175 mediates invasion in Plasmodium falciparum utilizing sialic acid-dependent and -independent pathways. Proc. Natl. Acad. Sci. USA *100*, 4796–4801.

Duraisingh, M.T., Triglia, T., Ralph, S.A., Rayner, J.C., Barnwell, J.W., McFadden, G.I., and Cowman, A.F. (2003b). Phenotypic variation of Plasmodium falciparum merozoite proteins directs receptor targeting for invasion of human erythrocytes. EMBO J. *22*, 1047–1057.

Dvorak, J.A., Miller, L.H., Whitehouse, W.C., and Shiroishi, T. (1975). Invasion of erythrocytes by malaria merozoites. Science *187*, 748–750.

Dvorin, J.D., Bei, A.K., Coleman, B.I., and Duraisingh, M.T. (2010). Functional diversification between two related Plasmodium falciparum merozoite invasion ligands is determined by changes in the cytoplasmic domain. Mol. Microbiol. *75*, 990–1006.

Gilson, P.R., and Crabb, B.S. (2009). Morphology and kinetics of the three distinct phases of red blood cell invasion by Plasmodium falciparum merozoites. Int. J. Parasitol. *39*, 91–96.

Glushakova, S., Yin, D., Li, T., and Zimmerberg, J. (2005). Membrane transformation during malaria parasite release from human red blood cells. Curr. Biol. *15*, 1645–1650.

Hakansson, S., Charron, A.J., and Sibley, L.D. (2001). Toxoplasma evacuoles: a two-step process of secretion and fusion forms the parasitophorous vacuole. EMBO J. *20*, 3132–3144.

Harris, K.S., Casey, J.L., Coley, A.M., Masciantonio, R., Sabo, J.K., Keizer, D.W., Lee, E.F., McMahon, A., Norton, R.S., Anders, R.F., et al. (2005a). Binding hot spot for invasion inhibitory molecules on Plasmodium falciparum apical membrane antigen 1. Infect. Immun. *73*, 6981–6989.

Harris, P.K., Yeoh, S., Dluzewski, A.R., O'Donnell, R.A., Withers-Martinez, C., Hackett, F., Bannister, L.H., Mitchell, G.H., and Blackman, M.J. (2005b). Molecular identification of a malaria merozoite surface sheddase. PLoS Pathog. *1*, 241–251.

Howell, S.A., Well, I., Fleck, S.L., Kettleborough, C., Collins, C.R., and Blackman, M.J. (2003). A single malaria merozoite serine protease mediates shedding of multiple surface proteins by juxtamembrane cleavage. J. Biol. Chem. *278*, 23890–23898.

Ladda, R., Aikawa, M., and Sprinz, H. (1969). Penetration of erythrocytes by merozoites of mammalian and avian malarial parasites. J. Parasitol. *55*, 633–644.

Lauer, S., VanWye, J., Harrison, T., McManus, H., Samuel, B.U., Hiller, N.L., Mohandas, N., and Haldar, K. (2000). Vacuolar uptake of host components, and a role for cholesterol and sphingomyelin in malarial infection. EMBO J. *19*, 3556–3564.

Lebrun, M., Michelin, A., El Hajj, H., Poncet, J., Bradley, P.J., Vial, H., and Dubremetz, J.F. (2005). The rhoptry neck protein RON4 re-localizes at the moving junction during Toxoplasma gondii invasion. Cell. Microbiol. *7*, 1823–1833.

Leykauf, K., Treeck, M., Gilson, P.R., Nebl, T., Braulke, T., Cowman, A.F., Gilberger, T.W., and Crabb, B.S. (2010). Protein kinase a dependent phosphorylation of apical membrane antigen 1 plays an important role in erythrocyte invasion by the malaria parasite. PLoS Pathog. *6*, e1000941.

Lingelbach, K., and Joiner, K.A. (1998). The parasitophorous vacuole membrane surrounding Plasmodium and Toxoplasma: an unusual compartment in infected cells. J. Cell Sci. *111*, 1467–1475.

Miller, L.H., Aikawa, M., Johnson, J.G., and Shiroishi, T. (1979). Interaction between cytochalasin B-treated malarial parasites and erythrocytes. Attachment and junction formation. J. Exp. Med. *149*, 172–184.

Mital, J., Meissner, M., Soldati, D., and Ward, G.E. (2005). Conditional expression of Toxoplasma gondii apical membrane antigen-1 (TgAMA1) demonstrates that TgAMA1 plays a critical role in host cell invasion. Mol. Biol. Cell *16*, 4341–4349.

Mitchell, G.H., Thomas, A.W., Margos, G., Dluzewski, A.R., and Bannister, L.H. (2004). Apical membrane antigen 1, a major malaria vaccine candidate, mediates the close attachment of invasive merozoites to host red blood cells. Infect. Immun. *72*, 154–158.

O'Donnell, R.A., and Blackman, M.J. (2005). The role of malaria merozoite proteases in red blood cell invasion. Curr. Opin. Microbiol. *8*, 422–427.

Richard, D., Kats, L.M., Langer, C., Black, C.G., Mitri, K., Boddey, J.A., Cowman, A.F., and Coppel, R.L. (2009). Identification of rhoptry trafficking determinants and evidence for a novel sorting mechanism in the malaria parasite Plasmodium falciparum. PLoS Pathog. *5*, e1000328.

Richard, D., MacRaild, C.A., Riglar, D.T., Chan, J.A., Foley, M., Baum, J., Ralph, S.A., Norton, R.S., and Cowman, A.F. (2010). Interaction between Plasmodium falciparum apical membrane antigen 1 and the rhoptry neck protein complex defines a key step in the erythrocyte invasion process of malaria parasites. J. Biol. Chem. *285*, 14815–14822.

Richards, J.S., and Beeson, J.G. (2009). The future for blood-stage vaccines against malaria. Immunol. Cell Biol. *87*, 377–390.

Rug, M., Wickham, M.E., Foley, M., Cowman, A.F., and Tilley, L. (2004). Correct promoter control is needed for trafficking of the ring-infected erythrocyte surface antigen to the host cytosol in transfected malaria parasites. Infect. Immun. *72*, 6095–6105.

Schermelleh, L., Carlton, P.M., Haase, S., Shao, L., Winoto, L., Kner, P., Burke, B., Cardoso, M.C., Agard, D.A., Gustafsson, M.G., et al. (2008). Subdiffraction multicolor imaging of the nuclear periphery with 3D structured illumination microscopy. Science *320*, 1332–1336.

Schofield, L., Bushell, G.R., Cooper, J.A., Saul, A.J., Upcroft, J.A., and Kidson, C. (1986). A rhoptry antigen of Plasmodium falciparum contains conserved and variable epitopes recognized by inhibitory monoclonal antibodies. Mol. Biochem. Parasitol. *18*, 183–195.

Singh, A.P., Ozwara, H., Kocken, C.H., Puri, S.K., Thomas, A.W., and Chitnis, C.E. (2005). Targeted deletion of Plasmodium knowlesi Duffy binding protein confirms its role in junction formation during invasion. Mol. Microbiol. *55*, 1925–1934.

Singh, S., Alam, M.M., Pal-Bhowmick, I., Brzostowski, J.A., and Chitnis, C.E. (2010). Distinct external signals trigger sequential release of apical organelles during erythrocyte invasion by malaria parasites. PLoS Pathog. *6*, e1000746.

Snow, R.W., Guerra, C.A., Noor, A.M., Myint, H.Y., and Hay, S.I. (2005). The global distribution of clinical episodes of Plasmodium falciparum malaria. Nature *434*, 214–217.

Sterkers, Y., Scheidig, C., da Rocha, M., Lepolard, C., Gysin, J., and Scherf, A. (2007). Members of the low-molecular-mass rhoptry protein complex of Plasmodium falciparum bind to the surface of normal erythrocytes. J. Infect. Dis. *196*, 617–621.

Straub, K.W., Cheng, S.J., Sohn, C.S., and Bradley, P.J. (2009). Novel components of the Apicomplexan moving junction reveal conserved and coccidia-restricted elements. Cell. Microbiol. *11*, 590–603.

Stubbs, J., Simpson, K.M., Triglia, T., Plouffe, D., Tonkin, C.J., Duraisingh, M.T., Maier, A.G., Winzeler, E.A., and Cowman, A.F. (2005). Molecular mechanism for switching of P. falciparum invasion pathways into human erythrocytes. Science *309*, 1384–1387.

Torii, M., Adams, J.H., Miller, L.H., and Aikawa, M. (1989). Release of merozoite dense granules during erythrocyte invasion by Plasmodium knowlesi. Infect. Immun. *57*, 3230–3233.

Treeck, M., Zacherl, S., Herrmann, S., Cabrera, A., Kono, M., Struck, N.S., Engelberg, K., Haase, S., Frischknecht, F., Miura, K., et al. (2009). Functional analysis of the leading malaria vaccine candidate AMA-1 reveals an essential role for the cytoplasmic domain in the invasion process. PLoS Pathog. *5*, e1000322.

Triglia, T., Healer, J., Caruana, S.R., Hodder, A.N., Anders, R.F., Crabb, B.S., and Cowman, A.F. (2000). Apical membrane antigen 1 plays a central role in erythrocyte invasion by Plasmodium species. Mol. Microbiol. *38*, 706–718.